Theranostic ultrasound-facilitated magnetogenetics

Alec J. Batts[1], Madhuvanthi Kannan[2], Ganesh Vasan[2], Daniel T. Hinojosa[3], Rebecca L. Noel[1], Jeannette Ingabire[4,5], Nancy Kwon[1], Vincent A. Pieribone[6,7,8], Qingbo Zhang[3], Jacob T. Robinson[3,4,9], and Elisa E. Konofagou[1,10]

[1]Dept. of Biomedical Engineering, Columbia University, New York, NY, USA; [2]Dept. of Neuroscience, University of Minnesota, Minneapolis, MN, USA; [3]Dept. Of Bioengineering, Rice University, Houston, TX, USA; [4]Dept. of Electrical and Computer Engineering, Rice University; [5]Systems, Synthetic and Physical Biology PhD Program, Rice University; [6]The John B. Pierce Laboratory, New Haven, CT, USA; [7]Dept. Of Cellular and Molecular Physiology, Yale University, New Haven, CT, USA; [9]Dept. of Neuroscience, Baylor College of Medicine, Houston, TX, USA; [10]Dept. of Radiology, Columbia University

Introduction

- Motivation: achieve non-invasive, remote brain-to-brain communication to minimize human communication latency (Fig. 1)
- Magnetogenetics enables minimally invasive and remote stimulation of neuronal targets deep within the brain [1-4]
  - **Magnetic nanoparticles** convert alternating magnetic fields (AMF) to heat [3]
  - Genetically encoded **thermoreceptors** convert local heat into neuronal action potentials [3, 5]
  - Addition of **genetically encoded voltage indicators (GEVI)** provides optical readout during stimulation [6]
- **Theranostic ultrasound (ThUS):** synchronous blood-brain barrier (BBB) opening and real-time power cavitation imaging using a repurposed diagnostic ultrasound transducer operating with short pulses [7-8]
  - Electronic beam steering enables multi-target BBB opening during a single sonication [8]
  - Exhibits faster BBB closing rate relative to long pulses, and delivers AAV across BBB [8]
  - Could be used for noninvasive delivery of magnetogenetic components

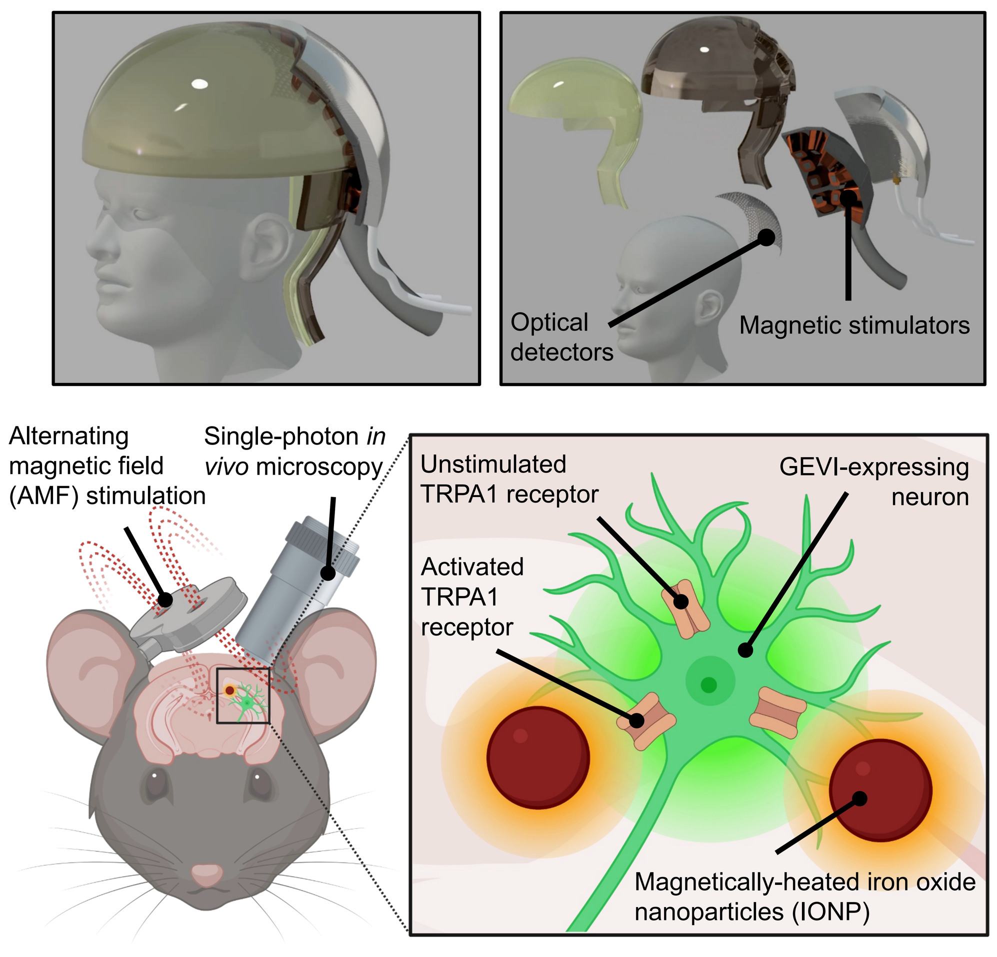

Figure 1: Magnetogenetic stimulation and recording in vivo. Top) Prototype of magnetogenetic-enabled brain-brain neuronal communication in humans. **Bottom)** Experimental overview of magnetogenetic stimulation in mice.

Objectives

- Optimize iron oxide nanoparticle (IONP) formulation for ThUS-mediated IONP delivery
- Develop viral vector constructs for ThUS-mediated BBB opening and evaluate expression of genetically encoded voltage indicators and TRPA1 thermoreceptors
- Demonstrate spatial colocalization of ThUS-delivered IONP and GEVI with multiple ThUS sessions

Methods

Theranostic Ultrasound (ThUS)

- **Single focus ThUS-mediated BBBO** with co-injected microbubbles and IONPs or AAV [7-8]

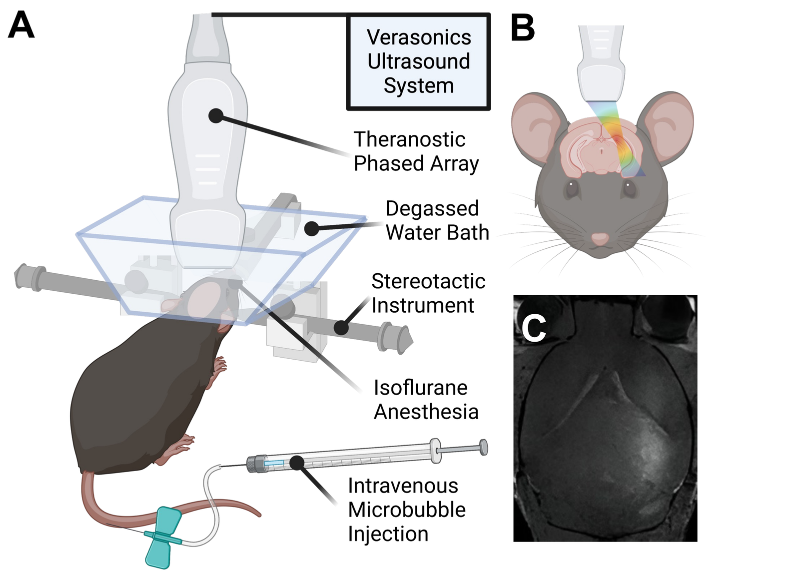

Figure 2: ThUS-mediated BBB opening. A) Experimental apparatus. **B)** Targeting and focusing achieved by electronic beam steering. **C)** Contrast-enhanced T_1-weighted MRI 20 acquired 20 minutes post-ThUS

Table 1: Single focus ThUS-mediated BBB opening parameters

Imaging Transducer	P4-1 (ATL, Philips)
Transmit Frequency	1.5 MHz
Bandwidth (-6 dB)	1.5 MHz – 3.5 MHz
Elements	96
Focal Depth	35 mm
Steering Angle	± 3.72 deg
Pulse Length	**10 cycles**
# of Sonications	1
Sonication Duration	2 min
Pulse Repetition Frequency	1000 Hz [7]
Peak Negative Pressure (derated)	**1.0 MPa**
Mechanical Index (MI)	**0.82**
Microbubbles	3.6e8 MBs/mL, Polydisperse, lipid shelled, perfluorobutane core

- **Multi focus ThUS-mediated BBBO** uses 9 distinct focal regions and low MI to induce sparse AAV delivery
- Whole-brain power cavitation imaging (PCI) displayed after segmentation of brain on pre-sonication B-mode image

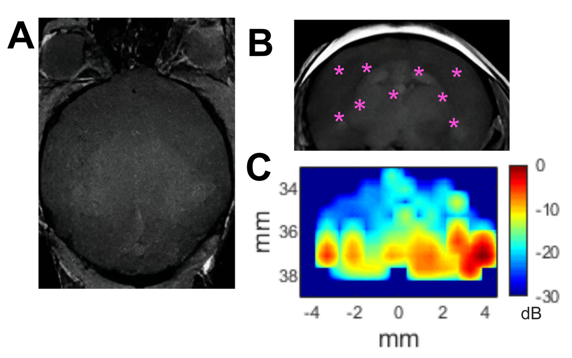

Figure 3: ThUS multi focus protocol. Axial **(A)** and coronal **(B)** Contrast-enhanced T_1-weighted MRI depicting locations of focal regions. **C)** Whole-brain cavitation mapping with power cavitation imaging (PCI)

Table 2: Multi focus TUS-mediated BBB opening parameters

Number of foci	9
Focal depth	various
Steering angle	various
Pulse Length	**1.5 cycles**
Peak Negative Pressure (derated)	**0.45 MPa**
Mechanical Index (MI)	**0.38**

Rate-sensitive thermoreceptors (TRPA1)

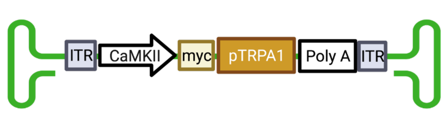

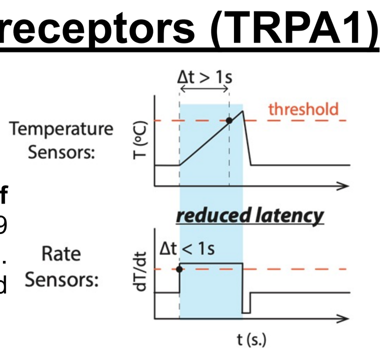

Figure 4: Plasmid and phenomenon of rate sensitive TRPA1. Above) AAV9 plasmid encoding rate-sensitive pTRPA1. **Right)** Rate sensors exhibit reduced latency relative to temperature sensors.

Table 3: Viral vector constructs for ThUS-mediated GEVI and TRPA1 delivery

	TRPA1	GEVI	
Construct	AAV9	AAVDJ	AAV9
Promoter	CaMKII	CAG	CaMKII
Transgene	pTRPA1	pACE or pACER	pACE
IV injected dose (gc/mouse)	1.3e11	1.3e11	1.1e11

Genetically-encoded voltage indicators (GEVI)

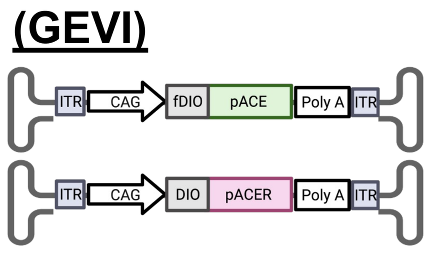

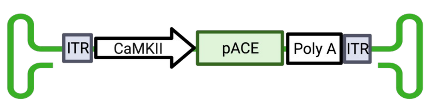

Figure 5: Viral vector plasmid components. Left) AAVDJ plasmids. **Above)** AAV9 plasmid

- pACE or pACER transgene fluorescence level correlates with neuronal spiking behavior [6]

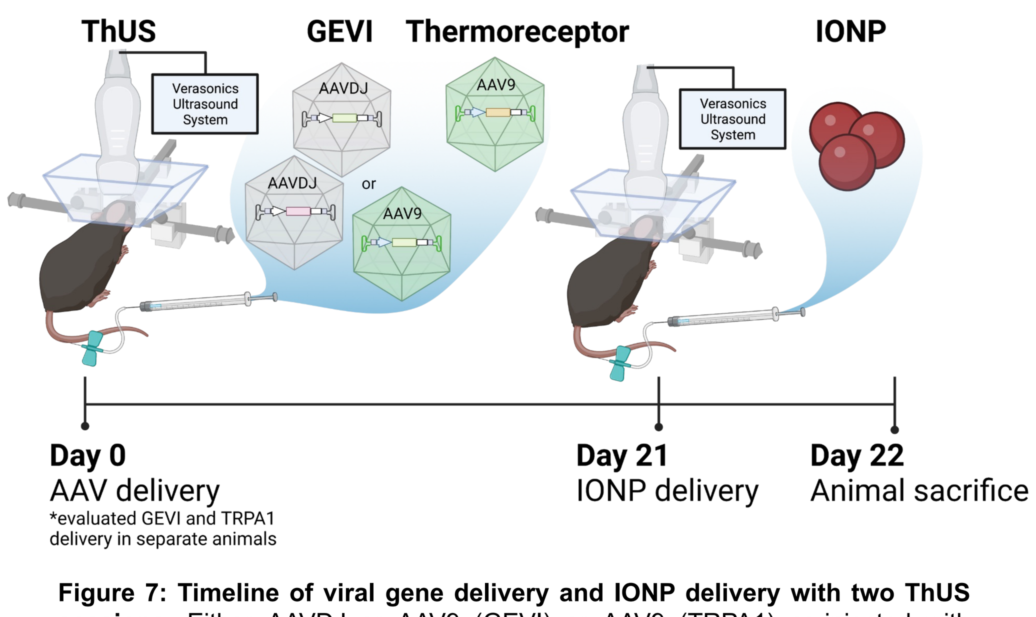

Figure 7: Timeline of viral gene delivery and IONP delivery with two ThUS sessions. Either AAVDJ or AAV9 (GEVI) or AAV9 (TRPA1) co-injected with microbubbles on day 0 for ThUS-mediated BBB opening. After 3-week transduction period, IONP delivered with second ThUS session on day 21, followed by sacrifice by transcardial perfusion on day 22.

Iron oxide nanoparticles (IONP)

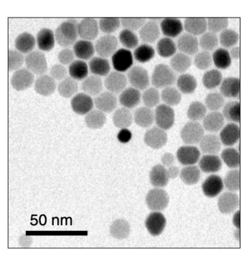

Figure 6: TEM image of 15 nm IONP [3]

Table 3: IONP properties

Chemical composition	Fe_3O_4
Diameter	15, 17, 19 nm
Diluent	5% dextrose
Fluorescent indicator	DiD
IV injected dose	5 mg/kg

Histology and microscopy

- Brains cryosectioned in coronal orientation at 35-μm thickness, and imaged with 10X or 20X magnification dry objectives with Leica DM5 or Olympus Microscope.

References

[1] Huang et al., *Nat. Nanotechnol.*, 2010
[2] Chen et al., *Science*, 2015
[3] Sebesta et al., *Nat. Mater.*, 2022
[4] Young et al., *Electron. Lett.*, 1980
[5] Wang et al., *J. Neural Eng.*, 2022
[6] Kannan & Vasan et al., *Science*, 2022
[7] Batts et al., *IEEE Trans. Biomed. Eng.*, 2022
[8] Batts et al., *Theranostics*, 2023

Acknowledgements

This study was funded in part by the National Institutes of Health (R01EB009041 and R01AG038961), the Naval Information Warfare Center (NIWC), and the Defense Advanced Research Projects Agency (DARPA) under Contract No. N66001-19-C-4020. The authors wish to thank the University of North Carolina Vector Core and Baylor University Vector Core for AAV synthesis.

Results

Reducing IONP diameter elicited increased deposition area of ThUS-delivered IONP

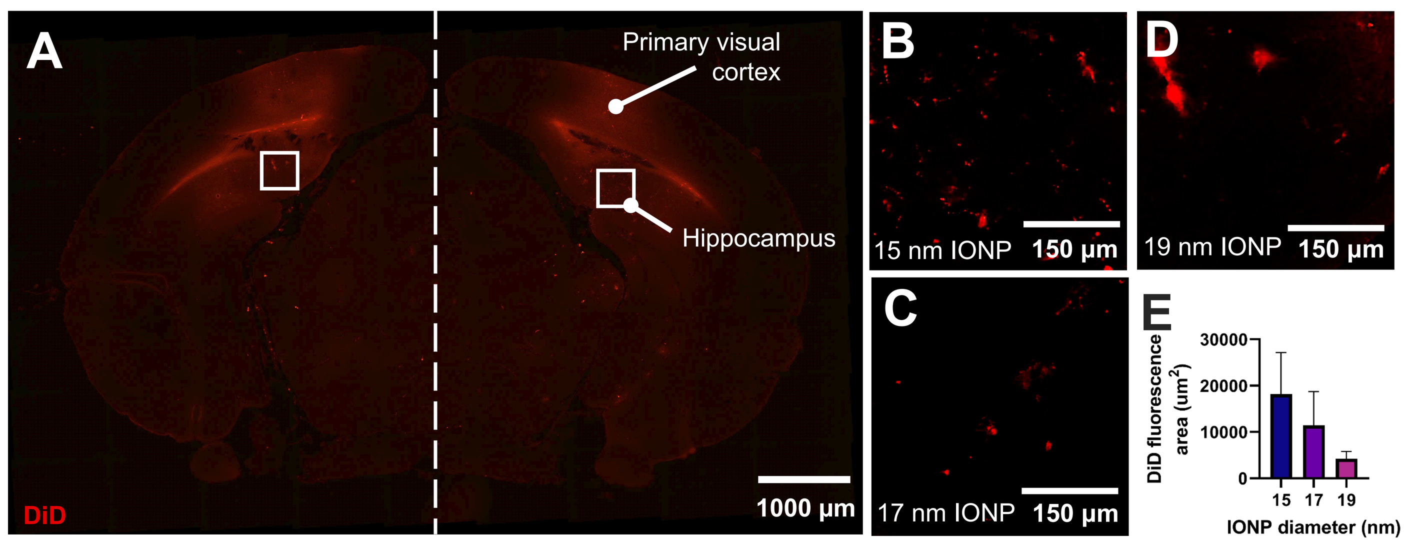

Figure 8: ThUS-facilitated iron-oxide nanoparticle (IONP) delivery. A) Entire coronal brain section demonstrating area of ThUS-delivered IONPs tagged with DiD dye. 15 nm IONP were delivered on the right hemisphere, while 19 nm IONP were delivered on the left hemisphere during a second sonication. Boxes denote the approximate ROIs of enlarged images in B-D. Representative images of 15 nm **(B),** 17 nm **(C)** and 19 nm **D)** IONP deposition. **E)** Quantification of area of IONP deposition vs. IONP diameter. Error bars denote mean ± standard deviation, n = 2 mice/group.

- Evaluated delivery of 3 different IONP diameters to optimize IONP formulation for ThUS-mediated BBB opening
- 17-19 nm IONP were more prone to aggregation (Fig. 8B-D), while 15 nm IONP exhibited 2.4- fold and 4.3-fold increased deposition area relative to 17 nm and 19 nm IONP, respectively (Fig. 8C-E)
- Thermal characterization is ongoing to determine magnetic heating capability of ThUS-delivered IONP

Optimization of AAV construct significantly increased ThUS-facilitated GEVI delivery

- AAVDJ-CAG-f/DIO-pACE (green) - pACER (red) exhibited poor neuronal specificity and overall transduction after ThUS-mediated BBBO (Fig. 9A-D,G)
- AAV9-CaMKII-pACE exhibited dramatically increased overall transduction and neuronal specificity relative to AAVDJ counterpart (Fig. 9E,G)
- Feasibility for recording sparse neuronal populations using low MI ThUS pulse sequence for AAV delivery (Fig. 9F)

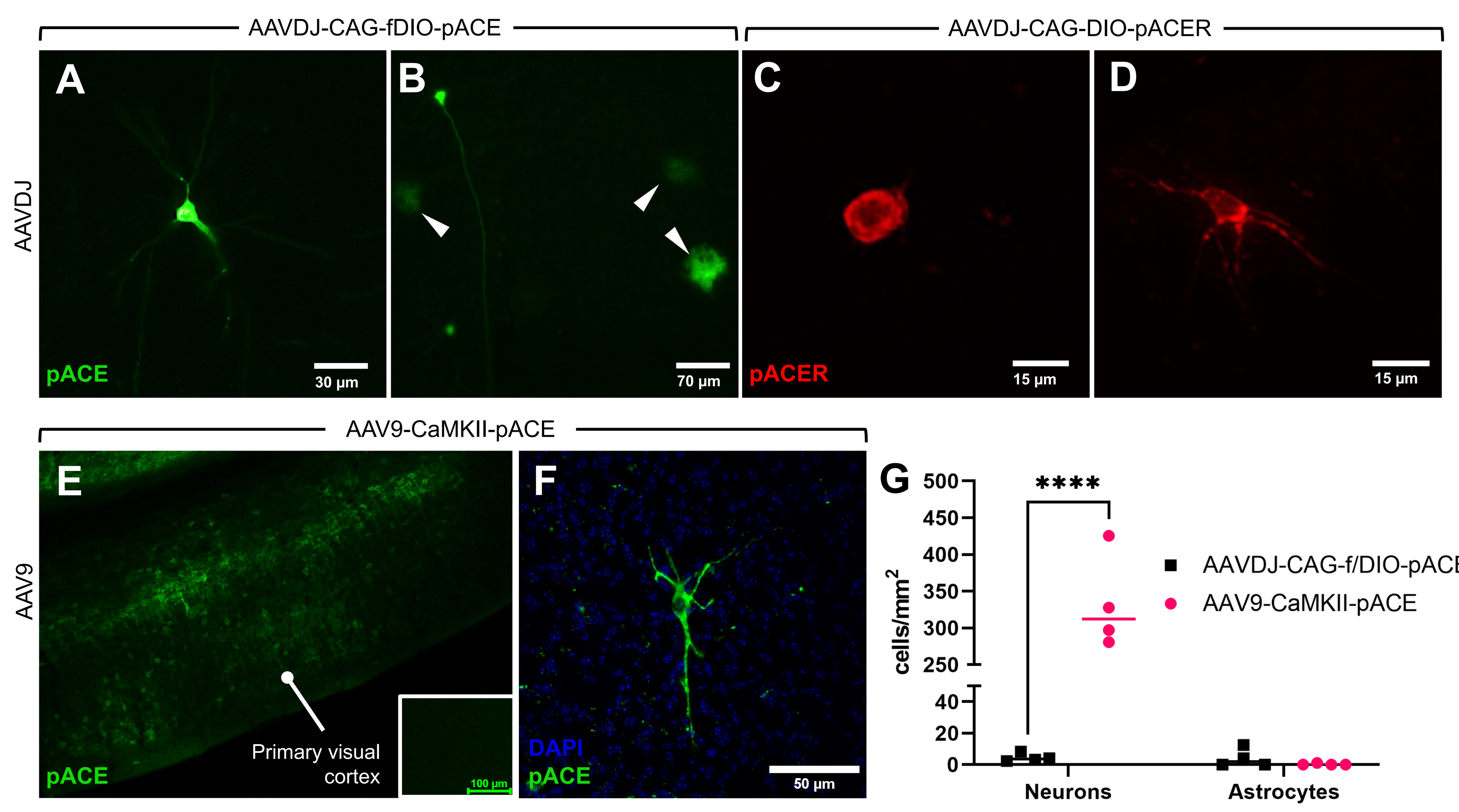

Figure 9: ThUS-facilitated genetically encoded voltage indicator (GEVI) delivery. Representative image of GEVI expression in neurons **(A)** and astrocytes **(B)** of pACE transgene driven by CAG promoter and encapsulated by AAVDJ serotype. White arrowheads denote transduced astrocytes. **C-D)** Representative image of GEVI expression in neurons of pACER transgene driven by CAG promoter and encapsulated by AAVDJ. **E)** Representative image of cortical pACE expression driven by CaMKII promoter and encapsulated in AAV9 capsid. Inset shows lack of GEVI expression on non-sonicated cortex. **F)** Singular pACE-expressing neuron transduced by lower MI ThUS pulse sequence. **G)** Quantification of construct dependent cell transduction. p<0.0001 determined by two-way ANOVA with post hoc Sidak multiple comparisons test, n=4 mice/group

ThUS-mediated viral gene delivery and expression of rate-sensitive TRPA1

- Delivered AAV9-CaMKII-myc-TRPA1 with analogous pulse sequence and target coordinates to IONP delivery
- Positive DAB signal indicates neurons expressing TRPA1 after ThUS BBBO (Fig. 10A)

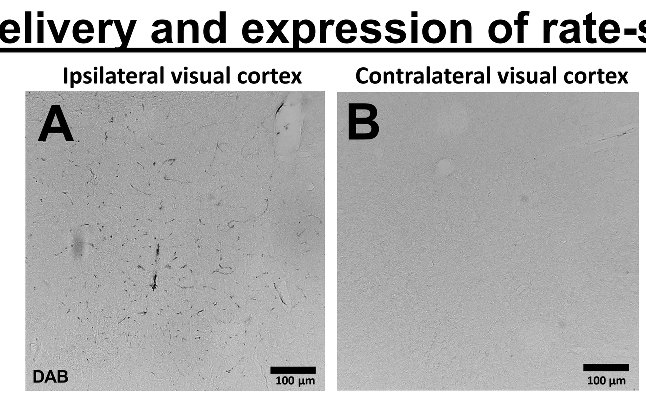

Figure 10: ThUS-facilitated TRPA1 delivery. A) Positive DAB staining (black) against myc tag encoded in AAV9-TRPA1 plasmid indicates TRPA1-expressing neurons located in ipsilateral sonicated visual cortex region approximately denoted in Fig. 8A. **B)** no detectable positive DAB signal in contralateral visual cortex.

Multiple sessions of ThUS mediated BBB opening elicited spatial colocalization of GEVI and IONP

- Mice received ThUS-mediated GEVI delivery on day 0, followed by survival for 21 days, ThUS-mediated IONP delivery at the same target on day 21, with sacrifice on day 22.
- Spatial colocalization of GEVI+ neurons and IONPs is possible with two ThUS sessions

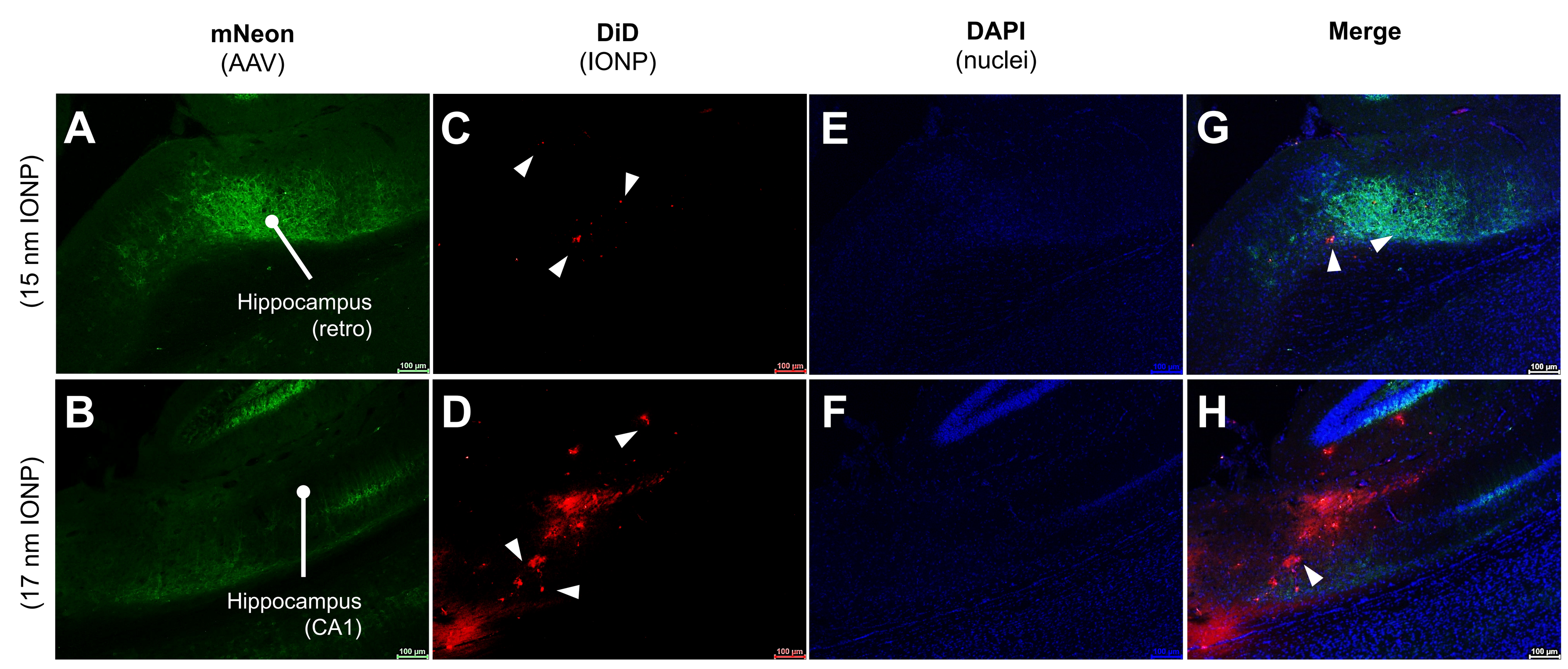

Figure 11: Spatial colocalization of IONP and GEVI-expressing neurons with repeated ThUS sonications. Representative subcortical pACE expression induced by AAV9-CamKII-pACE delivery on day 0 in mice which received 15 nm **(A)** IONP and 17 nm **(B)** IONP. Representative 15 nm **(C)** IONP and 17 nm **(D)** IONP deposition indicated by DiD fluorescence delivered with ThUS on day 21, with corresponding DAPI fluorescence denoting cell nuclei in **(E-F).** Merged channel images of spatial colocalization of pACE-expressing cells with 15 nm **(G)** IONP or 17 nm **(H)** IONP. Arrowheads denote regions where GEVI and IONP colocalization is observed.

Conclusions & Future Work

- Trending increase in ThUS-mediated IONP deposition observed with decreasing in IONP diameter (Fig. 8)
- ThUS-facilitated GEVI delivery with AAV9 capsid and CaMKII promoter exhibited significantly greater density and specificity of transduced neurons relative to AAVDJ constructs (Fig. 9)
- Single cell GEVI transduction per field of view achieved with low-MI, multi focus ThUS pulse sequence (Fig. 3, 9F)
- ThUS-optimized delivery of TRPA1 using AAV9 and CaMKII elicited neuronal expression of TRPA1 in vivo (Fig. 10)
- Spatial colocalization of AAV-mediated GEVI expression and IONP deposition is feasible with two sessions of ThUS (Fig. 11)

Ongoing and future work

- Thermal characterization of ThUS-delivered IONPs
- Long-term safety of IONP delivery
- *In vivo* GEVI imaging
- Synergistic behavioral experiment with ThUS-delivered NP, TRPA1, and GEVI
- ThUS-mediated AAV-TRPA1 delivery in NHP

MOANA

ajb2305@columbia.edu